Phenomenological and Predictability Studies of the Structure and Evolution of Arctic Cyclones, Polar Lows, and Tropopause Polar Vortices

Lance Bosart, Daniel Keyser, and Kevin Biernat

Department of Atmospheric and Environmental Sciences

University at Albany, State University of New York

Wednesday 30 May 2018

Research Supported by ONR Grant N00014-18-1-2200

Project Objective

- This project addresses three research topics concerned with improving prediction of Arctic cyclones and related phenomena in support of the ONR DRI entitled "Overcoming the Barrier to Extended Range Prediction over the Arctic."

- This project is expected to contribute to advances in the understanding and prediction of tropopause polar vortices (TPVs), Arctic cyclones, and polar lows on synoptic-to-subseasonal time scales.

Project Objective

- This project will be conducted by the PI (Lance Bosart), Co-PI (Dan Keyser), and two DAES graduate students (Kevin Biernat and Mansour Riachy) in collaboration with Steven Cavallo, Jim Doyle, Andrea Lang, and Ryan Torn, to leverage and benefit from their respective areas of expertise in addressing the project research topics.

Research Topics

1. The role of longitudinally localized incursions of warm, moist air from middle latitudes in disrupting the tropospheric polar vortex and in reconfiguring the large-scale baroclinicity over the Arctic.

2. The influence of reconfigurations of large-scale baroclinicity, high-latitude ridge amplification and blocking, sea ice and snow cover boundaries, and radiative processes on the genesis and evolution of TPVs, Arctic cyclones, and polar lows.

Research Topics

3. The dependence of predictability horizons of TPVs, Arctic cyclones, and polar lows on model uncertainty on synoptic-to-subseasonal time scales as determined through the synoptic evaluation of the forecast skill of deterministic and ensemble prediction systems.

- Research topic #3 will be emphasized, and research topics #1 and #2 will establish the phenomenological basis for research topic #3.

Research Topics

- Research topic #1 will be addressed by performing climatologies, composite analyses, and case studies of Arctic cyclones and the tropospheric polar vortex.

- Research topic #2 will be addressed by performing case studies and associated composite analyses of interactions between TPVs, Arctic cyclones, and polar lows.

- Research topic #3 will be addressed by performing predictability studies of TPVs, Arctic cyclones, and polar lows on synoptic-to-subseasonal time scales for episodes of compromised global model forecast skill.

Research Topics

- In addressing the three research topics, we will
  - Use reanalysis datasets, in conjunction with deterministic and ensemble forecasts, produced by the Navy.
  - Use MPAS (Model for Prediction Across Scales) in predictive and ensemble modes to investigate multiscale interactions between TPVs, Arctic cyclones, and polar lows.
  - Participate in the field program, THINICE.

Research Topics

- Participation in THINICE will consist of analysis and forecasting, as well as real-time monitoring, of evolving Arctic weather regimes and events applicable to the objectives and hypotheses to be addressed during selected intensive observing periods (IOPs).

- Conventional synoptic datasets and model forecasts, supplemented by applicable research datasets available during the IOPs, will be used to conduct the above analysis and forecasting, as well as monitoring, activities.

Research Topics

- Observations applicable to research topics:
  - Dropsonde observations suitable for obtaining cross-latitude fluxes of heat, moisture, momentum, and PV over specific longitudinal sectors (e.g., the Greenland Sea and Northeast Asia cyclone “freeways”) during anticipated midlatitude–polar interaction periods.
  - Measurements of vertical profiles of heat and moisture fluxes within the planetary boundary layer over open water, broken ice, and solid ice.
  - Dropsonde observations along the tracks of TPVs and their environments over significant portions of the TPV life cycle.

Research Topic #1

1. The role of longitudinally localized incursions of warm, moist air from middle latitudes in disrupting the tropospheric polar vortex and in reconfiguring the large-scale baroclinicity over the Arctic.

Fig. 1

(a)

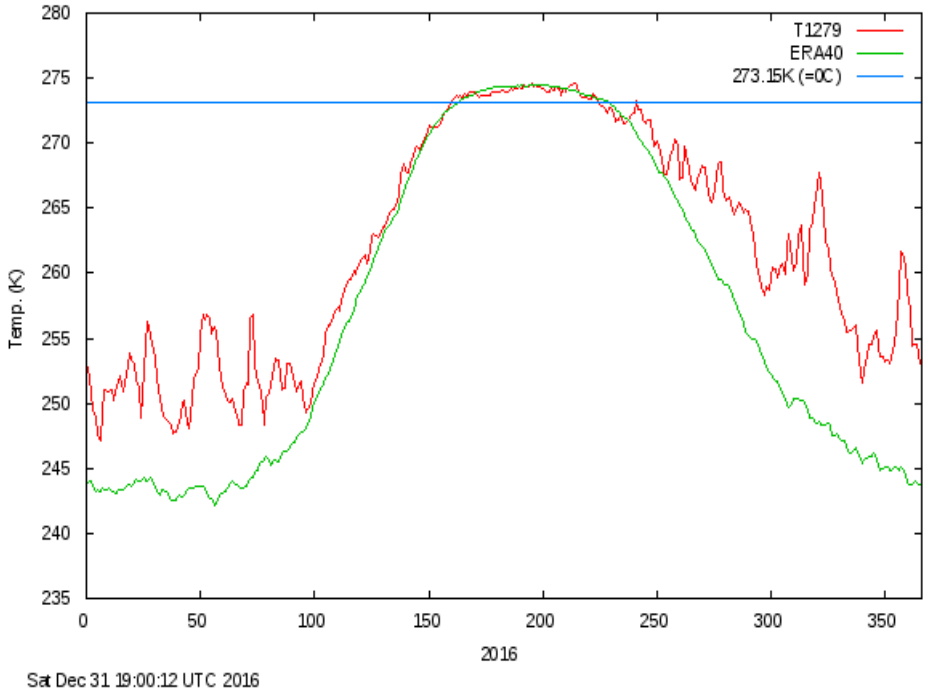

Daily mean Arctic temperatures poleward of 80°N. In addition to the astounding autumnal and winter warmth overall, the large temperature spikes in late November and December are noteworthy.

(b)

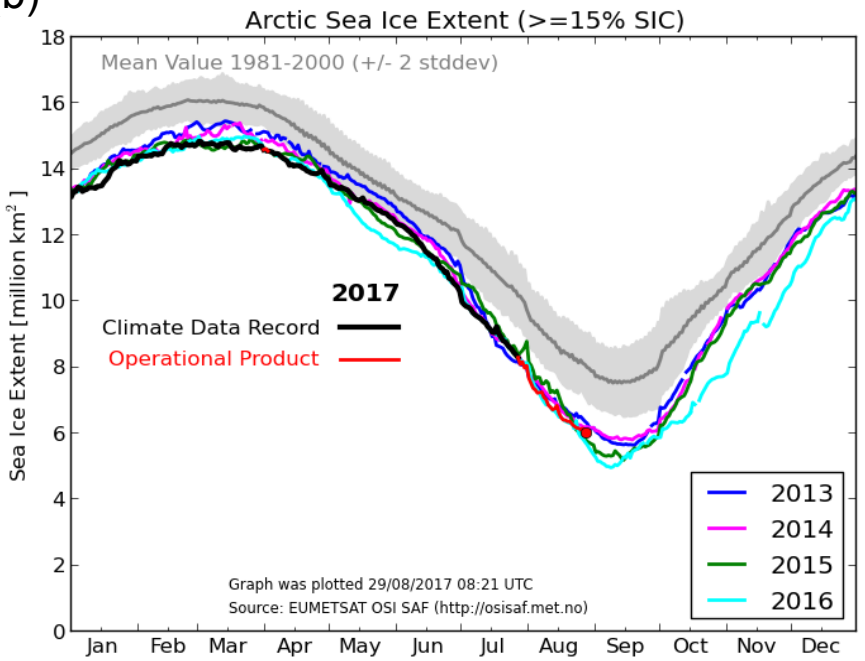

Arctic sea ice extent for 2013–2016. Note the small sea ice extent retreat during the time of the 2016 winter solstice.

Source: Danish Meteorological Institute (http://ocean.dmi.dk/arctic/meant80n.uk.php)

Research Topic #2

2. The influence of reconfigurations of large-scale baroclinicity, high-latitude ridge amplification and blocking, sea ice and snow cover boundaries, and radiative processes on the genesis and evolution of TPVs, Arctic cyclones, and polar lows.

Fig. 2

(a) tropopause pressure (hPa)

(b) Eady growth rate (day^{-1})

(c) 30 m s^{-1} jet frequency (%)

(d) cyclone frequency (%)

(e) blocking frequency (%)

(f) frequency of stratospheric potential vorticity (PV) cutoffs on 310 K (%)

(g) frequency of downward stratosphere–troposphere exchange (STE) trajectories (%)

(h) frequency of warm conveyor belt (WCB) trajectories (%)

(i) frequency of tropical moisture export (TME) trajectories (%)

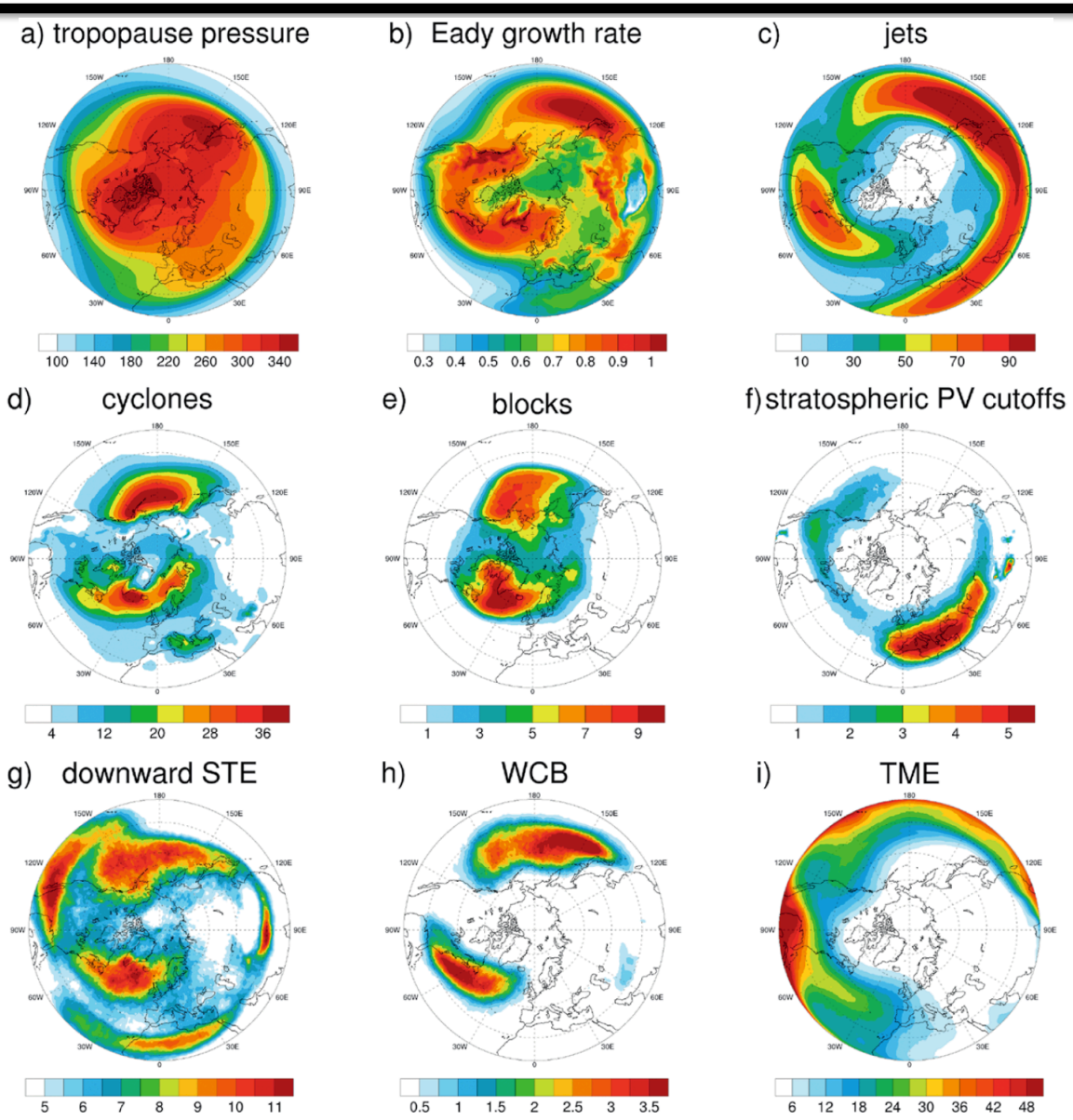

Climatological boreal winter fields in the Northern Hemisphere for 1979–2014 of quantities listed above. [Figure 1 and caption adapted from Sprenger et al. (2017).]

Research Topic #3

3. The dependence of predictability horizons of TPVs, Arctic cyclones, and polar lows on model uncertainty on synoptic-to-subseasonal time scales as determined through the synoptic evaluation of the forecast skill of deterministic and ensemble prediction systems.

Fig. 3

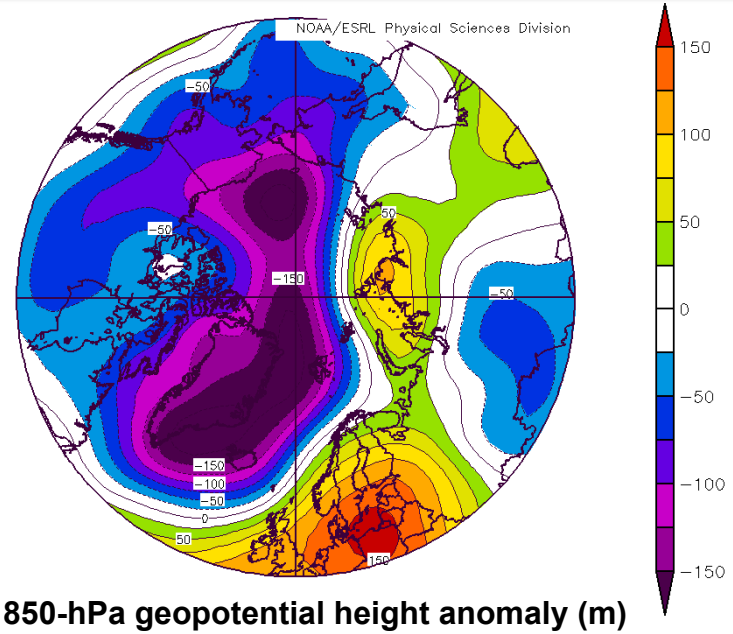

(a) 850-hPa geopotential height anomaly (m)

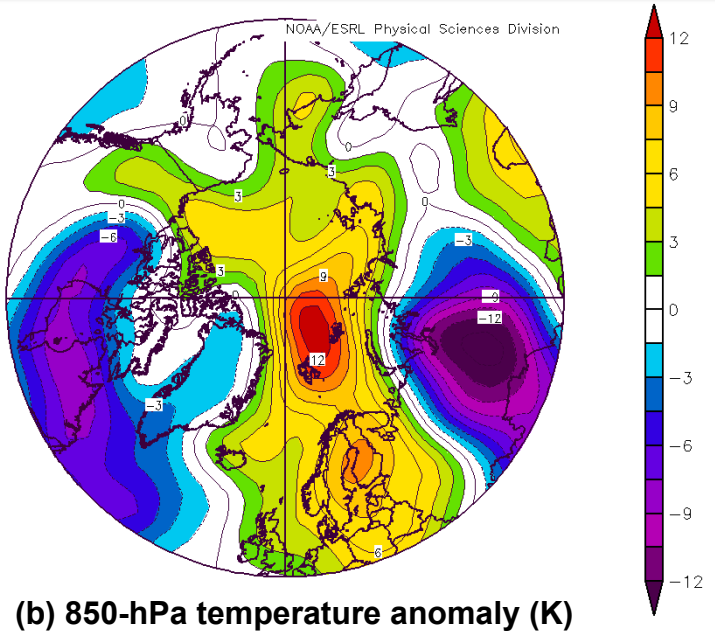

(b) 850-hPa temperature anomaly (K)

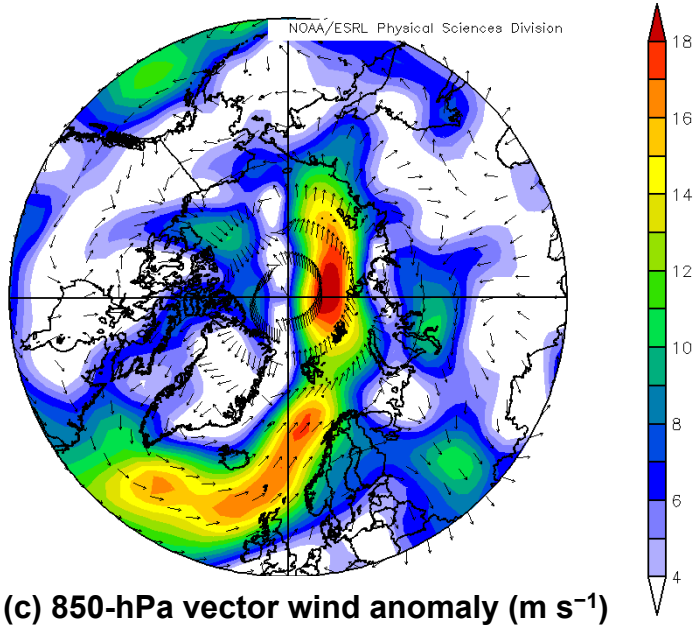

(c) 850-hPa vector wind anomaly (m s^{-1})

(a) 850-hPa geopotential height anomaly (m),
(b) 850-hPa temperature anomaly (K), and
(c) 850-hPa vector wind anomaly (m s^{-1})
for 17–23 December 2016,
from NCEP–NCAR Reanalysis.

Fig. 4

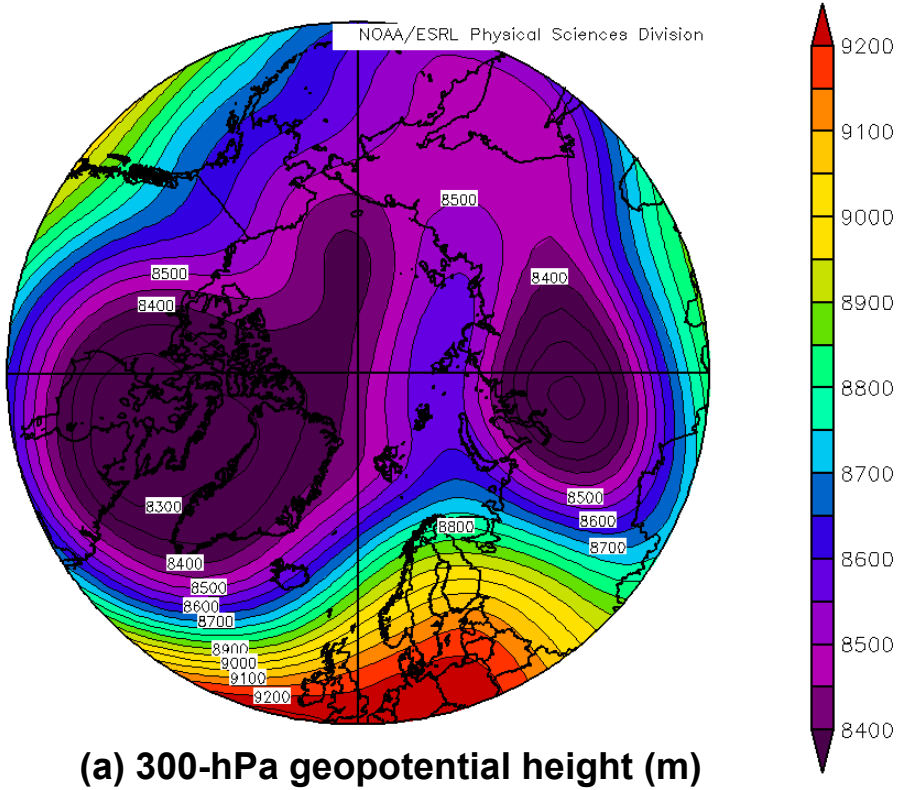

(a) 300-hPa geopotential height (m)

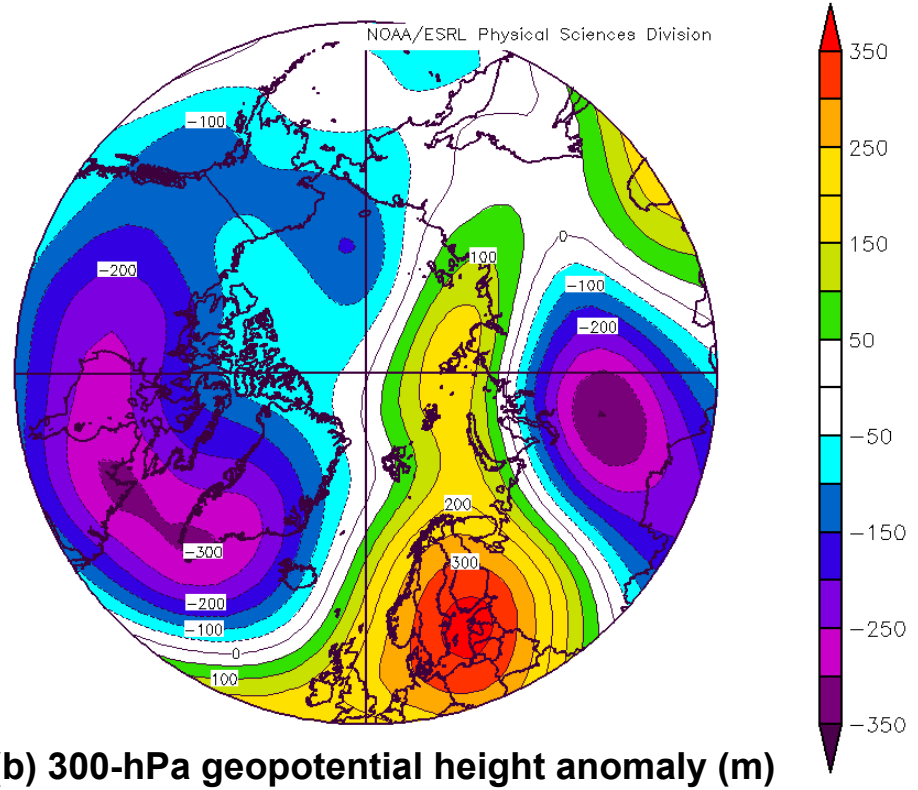

(b) 300-hPa geopotential height anomaly (m)

(a) 300-hPa geopotential height (m) and (b) 300-hPa geopotential height anomaly (m) for 17–23 December 2016, from NCEP–NCAR Reanalysis.

Fig. 5

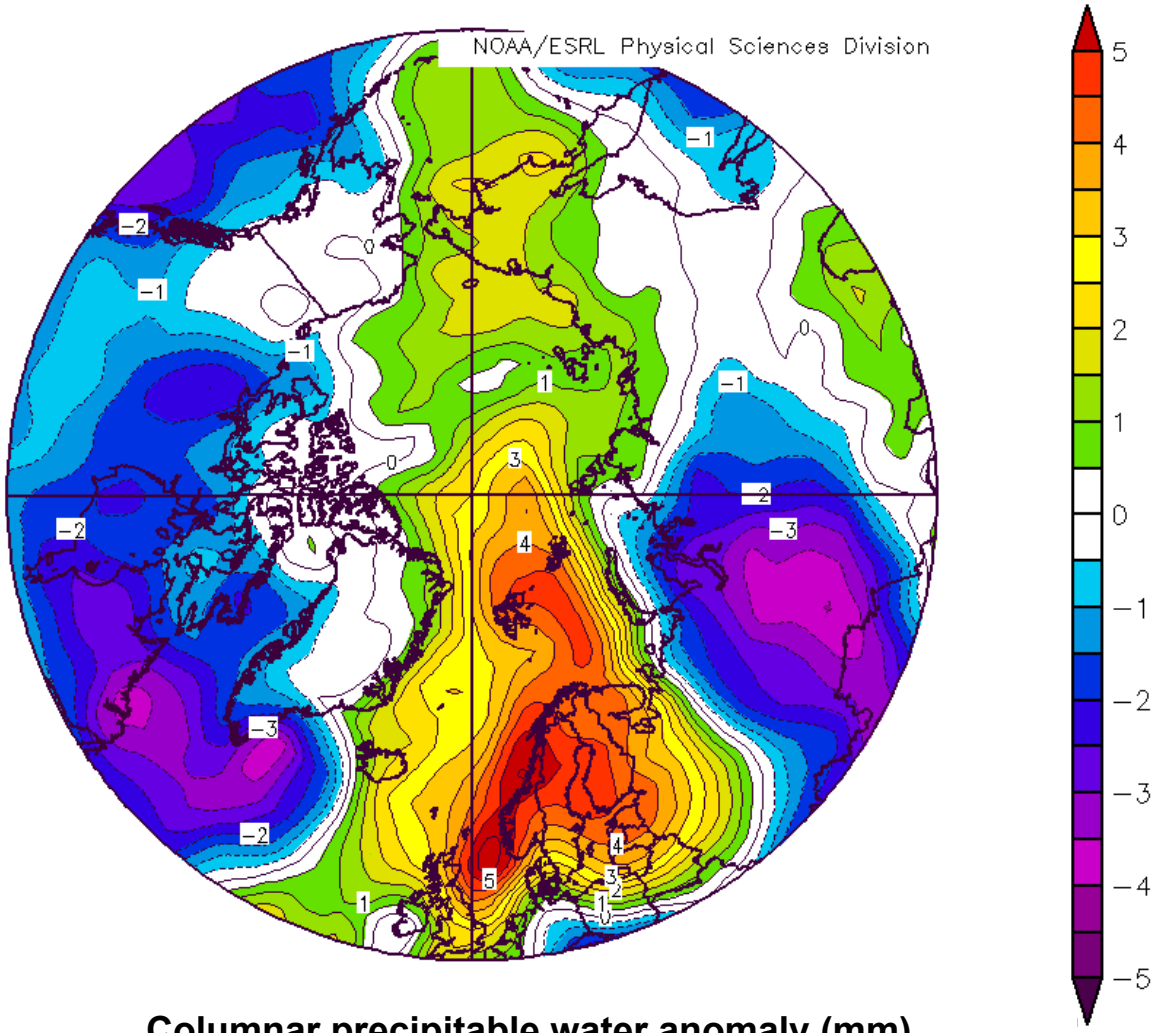

Columnar precipitable water anomaly (mm)

Columnar precipitable water anomaly (mm) for 17–23 December 2016, from NCEP–NCAR Reanalysis.

Research Topic #3

- A Multiscale Analysis and Predictability Study of a Polar Low Linked to a TPV

  - **The purpose of this study is to**

    1) Analyze the evolution of a polar low that is linked to a TPV.

    2) Investigate factors influencing the predictability of the evolution of the polar low.

Research Topic #3

- A Multiscale Analysis and Predictability Study of a Polar Low Linked to a TPV

  – A multiscale analysis is performed, using the ERA5, on a polar low that occurs during 10–11 February 2011 over the Barents Sea and is linked to a TPV transported equatorward along a tropospheric-deep baroclinic zone.

  – The analysis shows that the TPV and a favorable thermodynamic environment likely play an important role in supporting the development and intensification of the polar low.

Research Topic #3

- A Multiscale Analysis and Predictability Study of a Polar Low Linked to a TPV
  - The 51-member ECMWF Ensemble Prediction System (EPS) from TIGGE is utilized to evaluate forecast skill of the evolution of the polar low.
  - The ensemble members are separated in two groups: the most and least accurate members in terms of track and intensity errors of the polar low.

Research Topic #3

- A Multiscale Analysis and Predictability Study of a Polar Low Linked to a TPV
  - Composite differences between the most accurate and least accurate groups suggest that the TPV is positioned farther northward and the tropospheric-deep baroclinic zone farther eastward in the most accurate group.
  - The differences in position of the TPV and baroclinic zone likely contribute to a farther northward and eastward track of the polar low in the most accurate group.

Research Topic #3

- A Multiscale Analysis and Predictability Study of a Polar Low Linked to a TPV
  - The more conducive thermodynamic environment for polar low development in the most accurate group may contribute to the polar low being stronger in the most accurate group.

Fig. 6

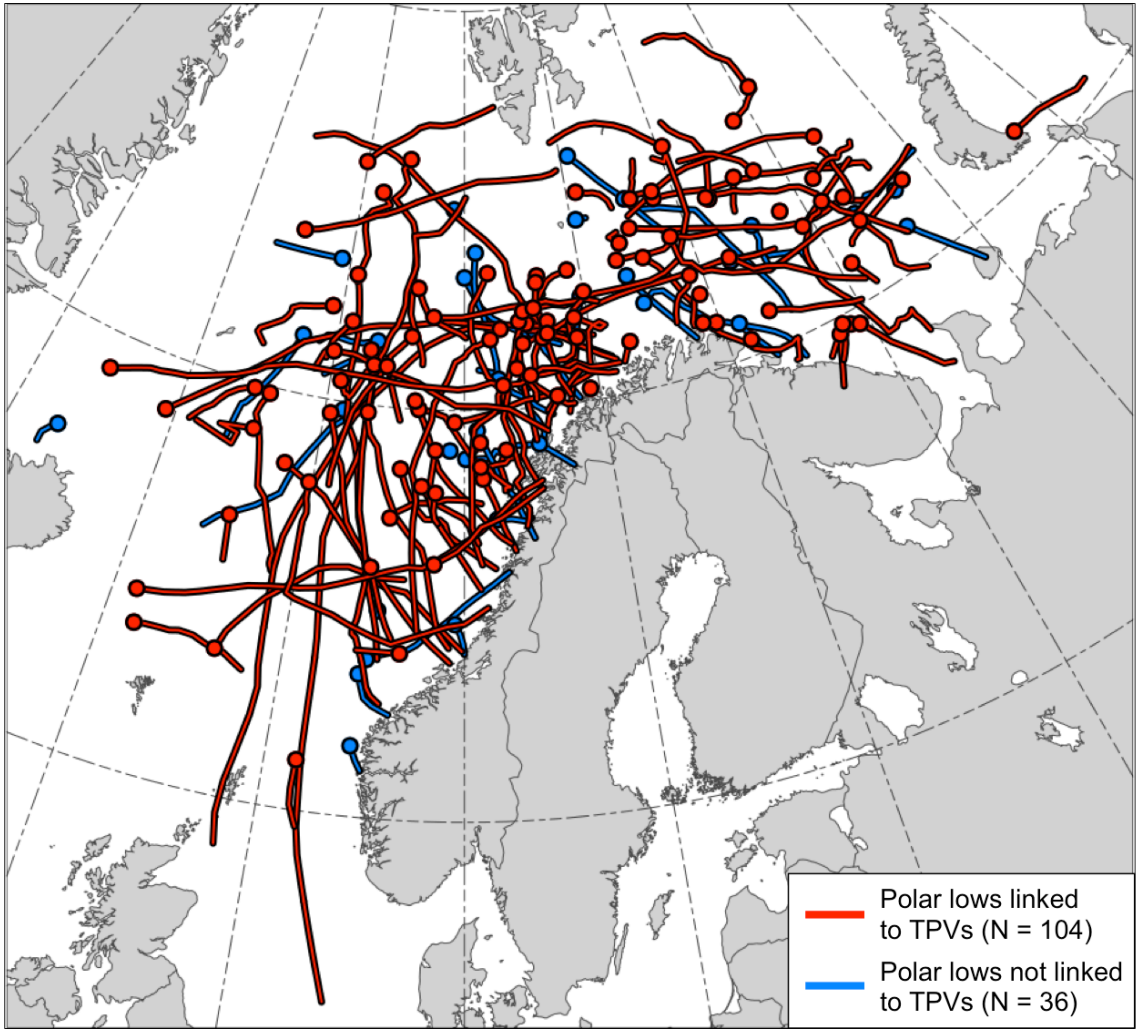

Tracks of the polar lows in the STARS database. Tracks of polar lows linked to TPVs (red) and tracks of polar lows not linked to TPVs (blue). Dots indicate the genesis locations of the polar lows.

Fig. 7

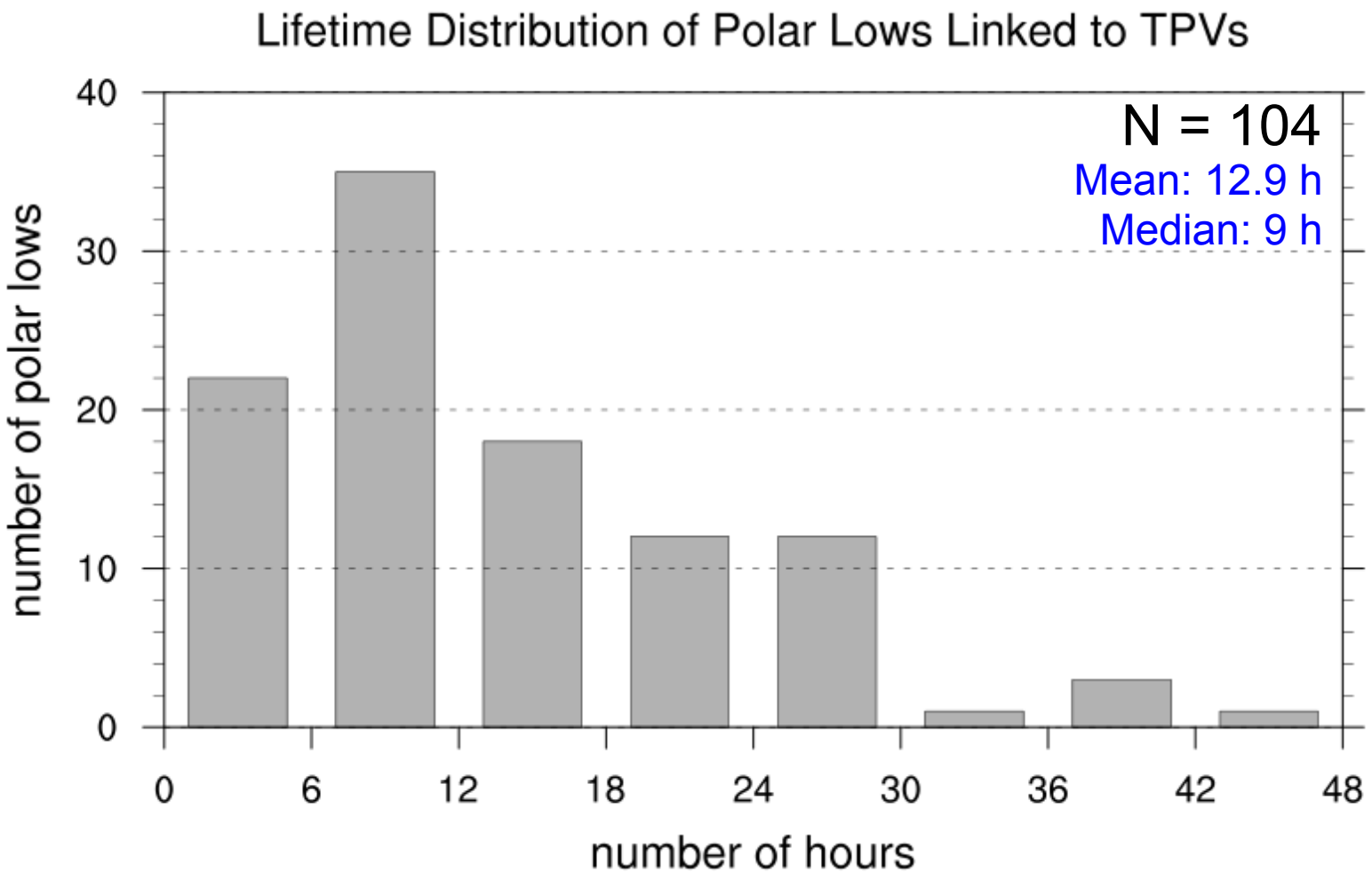

Lifetime distribution of polar lows linked to TPVs, with lifetime in number of hours.

Fig. 8

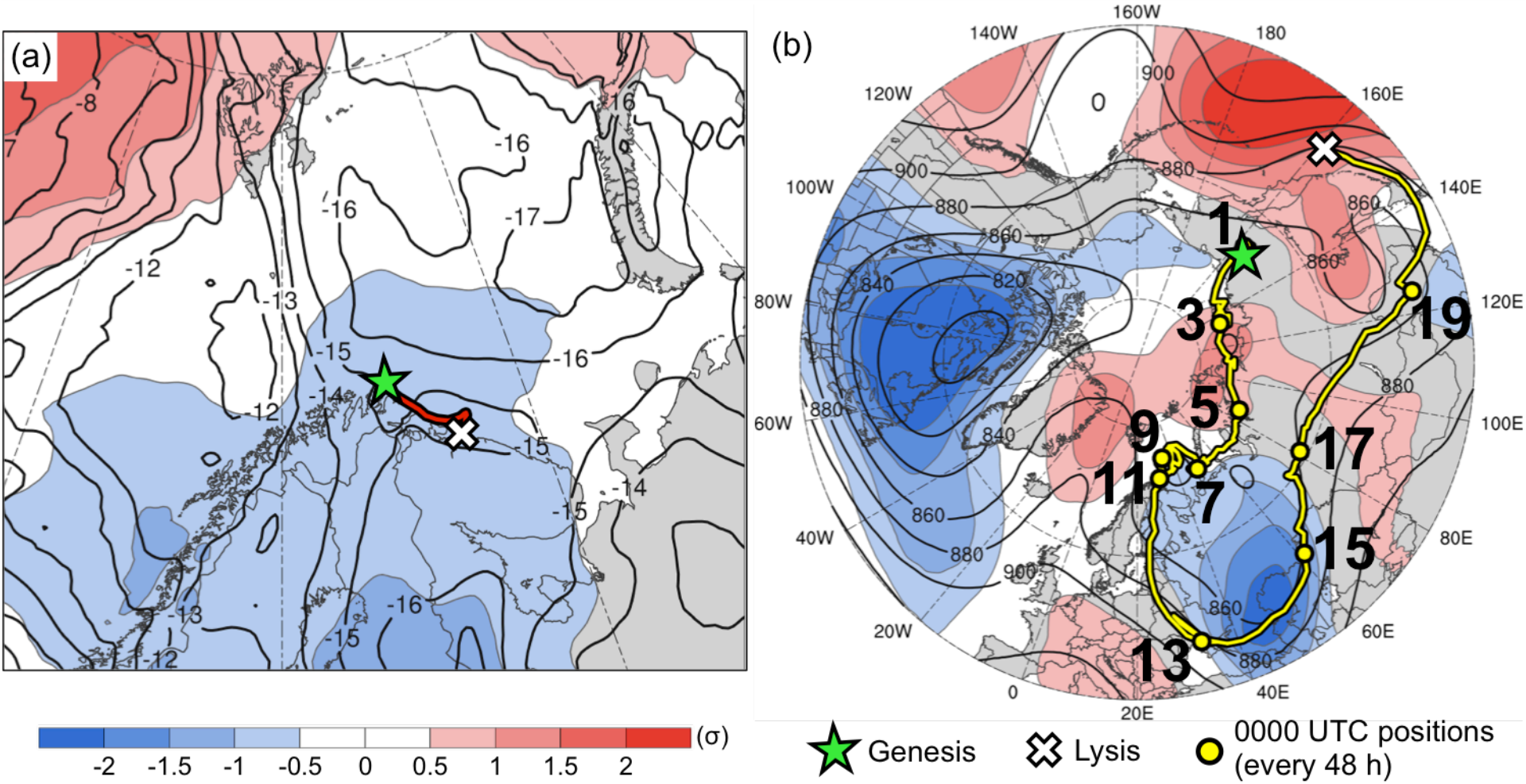

Feature	Genesis	Lysis	Lifetime
TPV	31 Jan	20 Feb	20 d
PL	10 Feb	11 Feb	18 h

Track of (a) polar low (red) and (b) TPV linked to the polar low (yellow). Also, the 10–11 February 2011 time-mean (a) 850-hPa temperature (K, black) and standardized anomaly of 850-hPa temperature (σ, shaded), and (b) 300-hPa geopotential height (dam) and standardized anomaly of 300-hPa geopotential height (σ, shaded).

Fig. 9

1800 UTC 10 Feb 2011

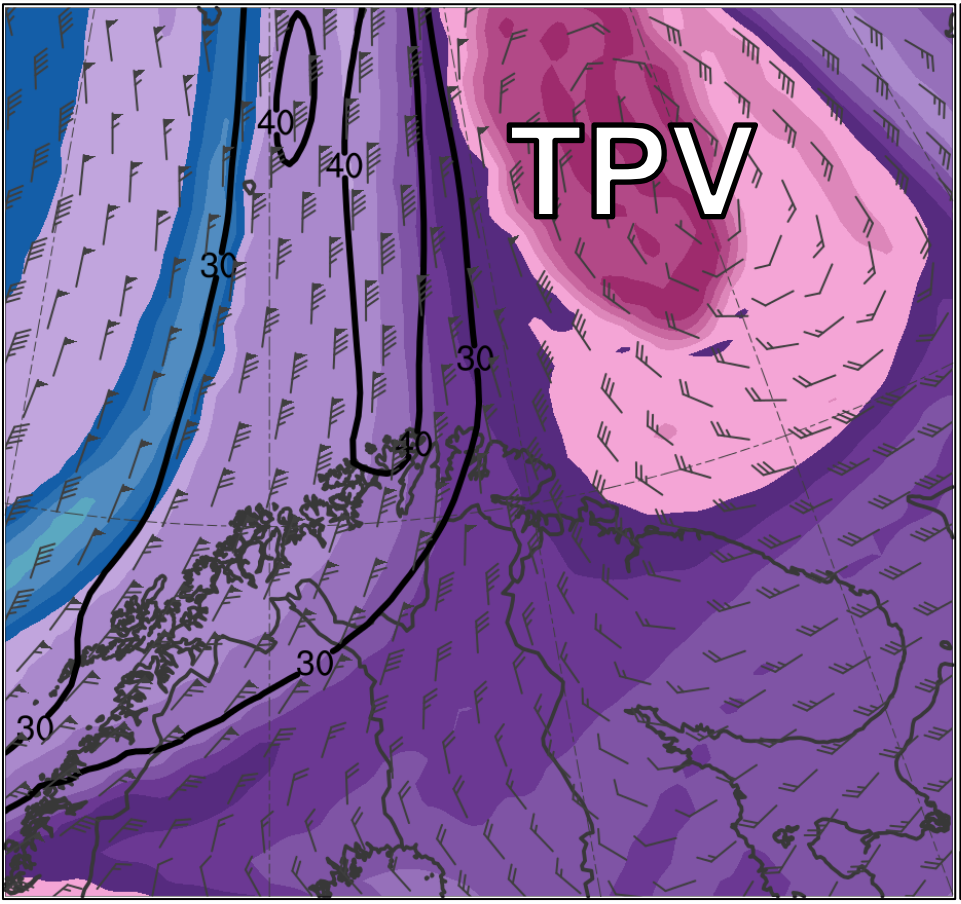

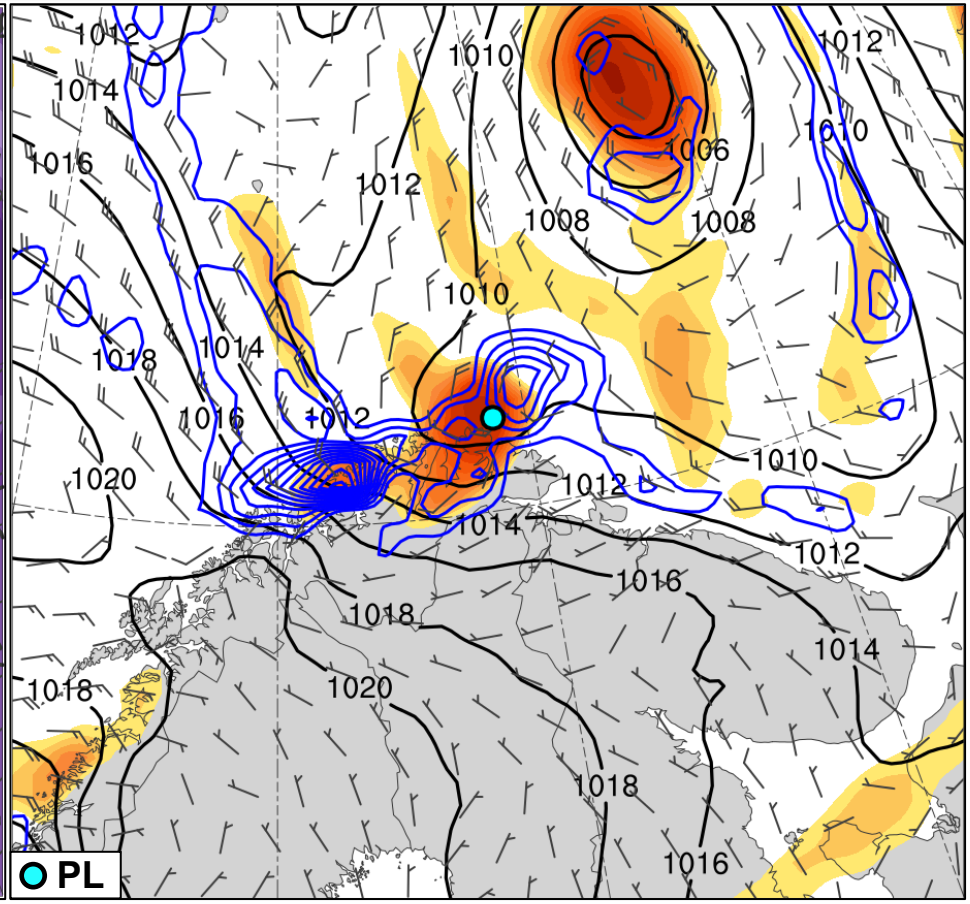

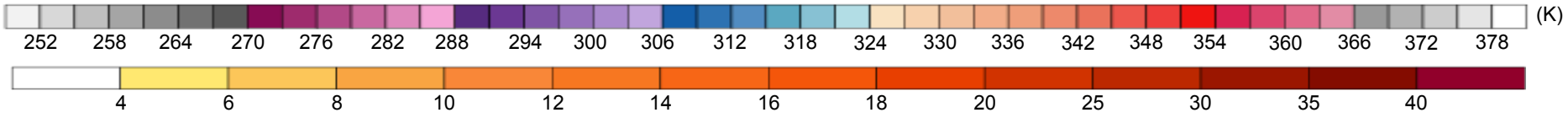

Potential temperature (K, shaded), wind speed (black, every 10 m s^{-1} starting at 30 m s^{-1}), and wind (m s^{-1}, flags and barbs) on 2-PVU surface

850-hPa relative vorticity (10^{-5} s^{-1}, shaded), 850–600-hPa ascent (blue, every 2.5 × 10^{-3} hPa s^{-1}), SLP (hPa, black), and 10-m wind (m s^{-1}, barbs)

Fig. 9

0000 UTC 11 Feb 2011

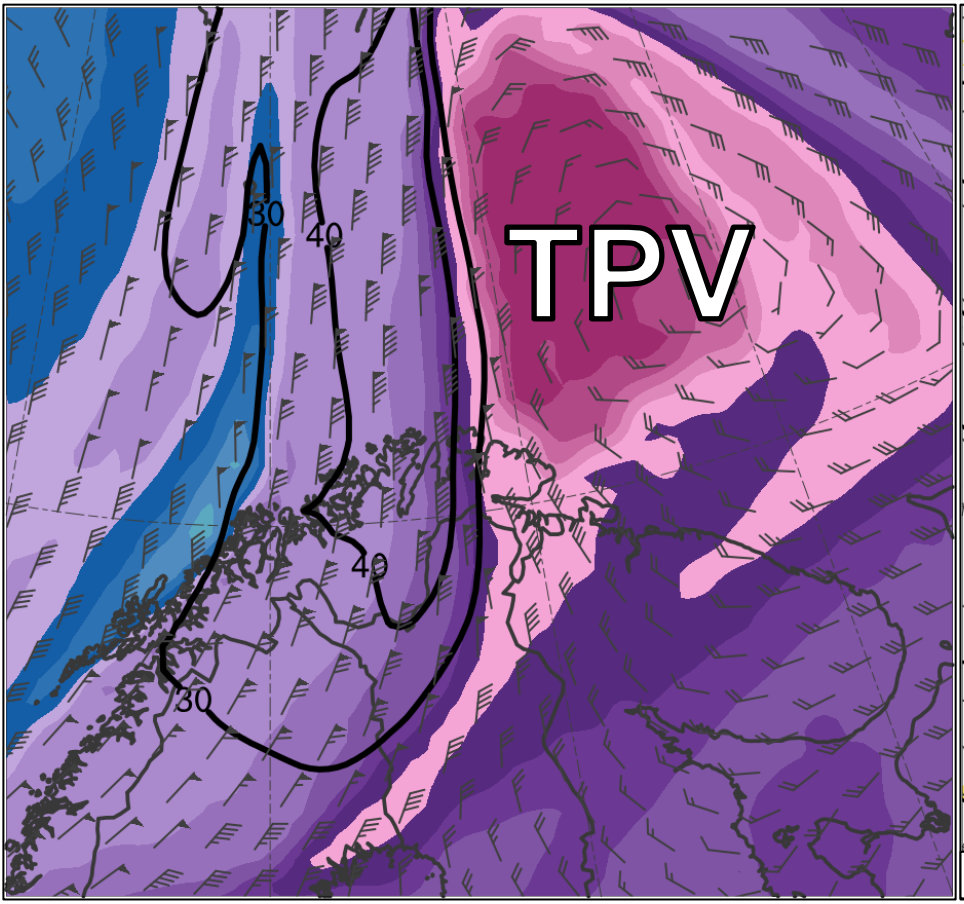

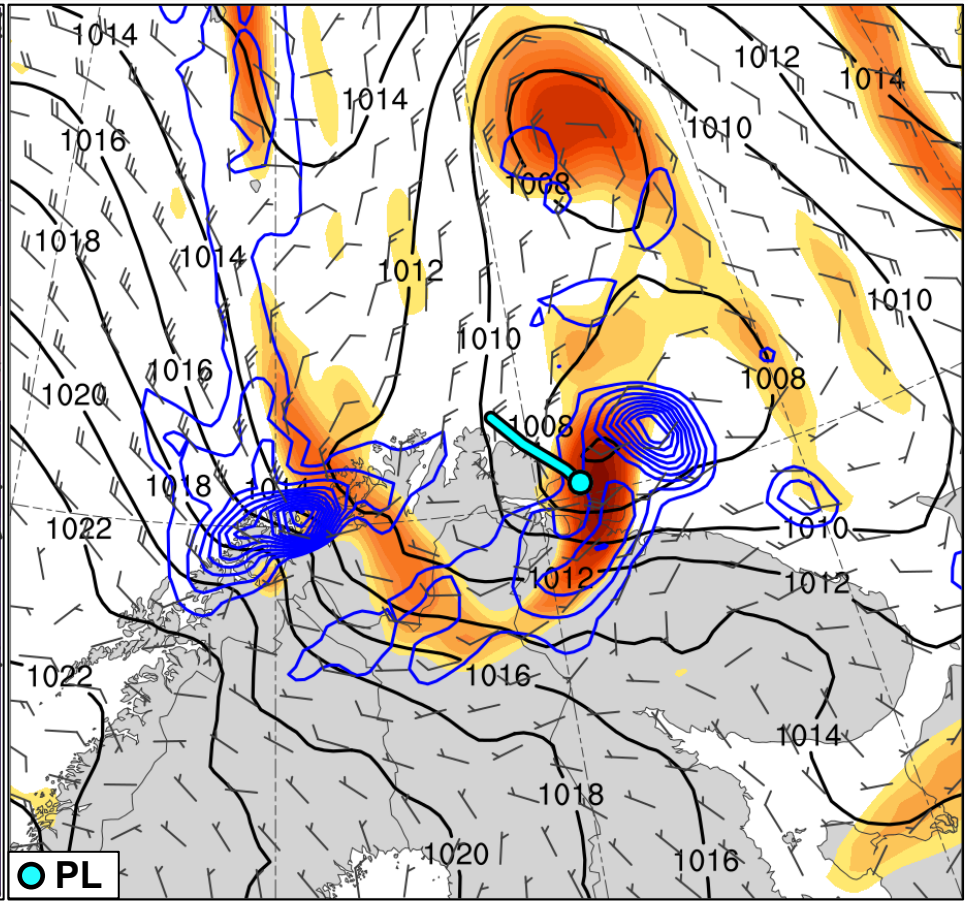

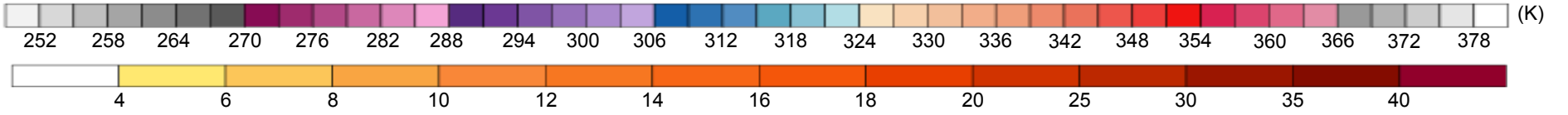

Potential temperature (K, shaded), wind speed (black, every 10 m s^{-1} starting at 30 m s^{-1}), and wind (m s^{-1}, flags and barbs) on 2-PVU surface

850-hPa relative vorticity (10^{-5} s^{-1}, shaded), 850–600-hPa ascent (blue, every 2.5 × 10^{-3} hPa s^{-1}), SLP (hPa, black), and 10-m wind (m s^{-1}, barbs)

Fig. 9

0600 UTC 11 Feb 2011

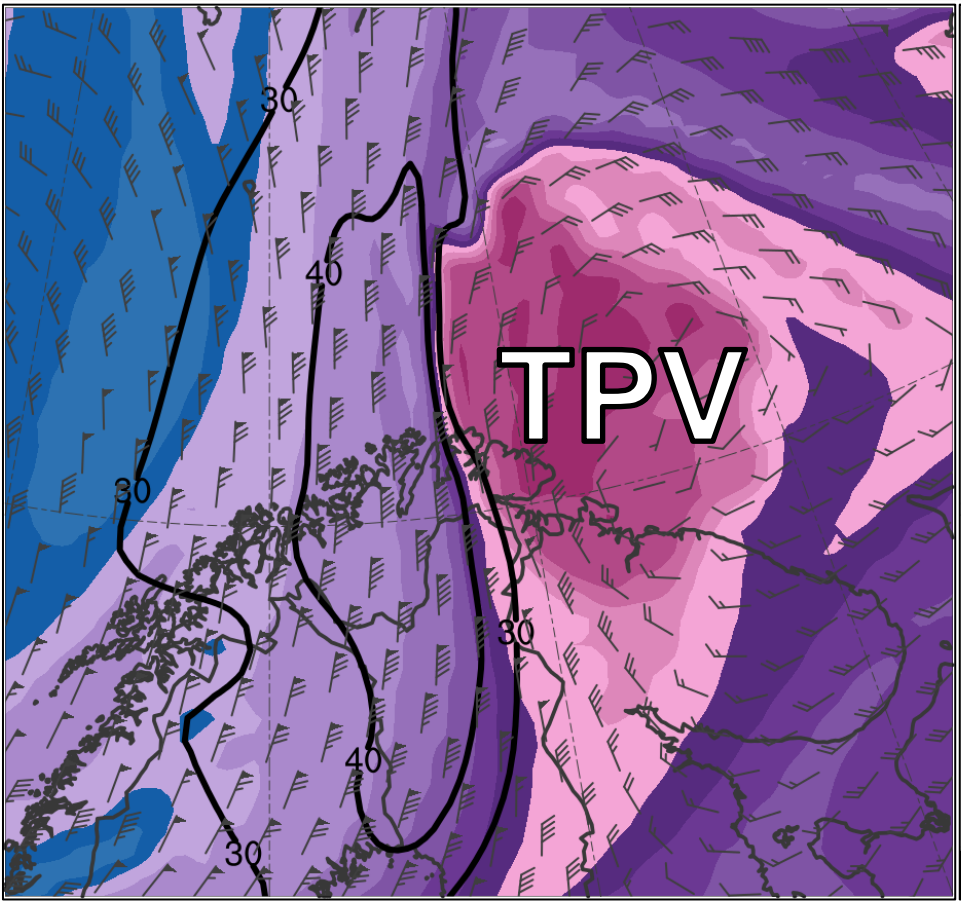

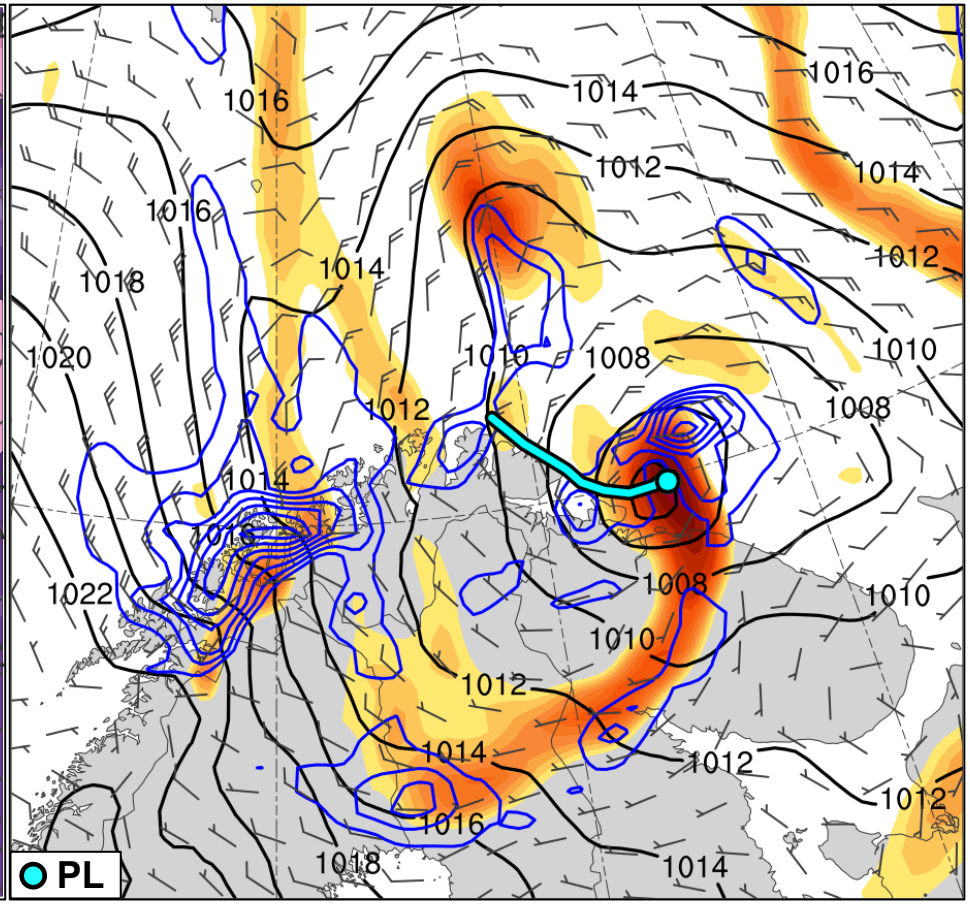

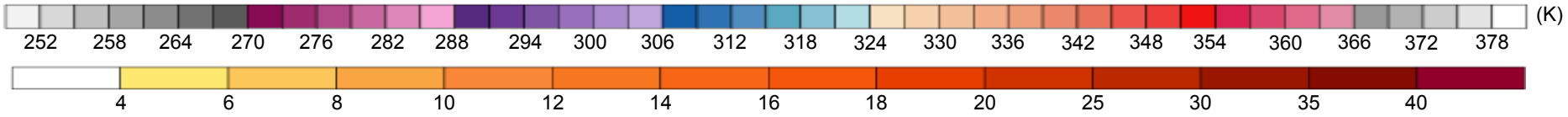

Potential temperature (K, shaded), wind speed (black, every 10 m s^{-1} starting at 30 m s^{-1}), and wind (m s^{-1}, flags and barbs) on 2-PVU surface

850-hPa relative vorticity (10^{-5} s^{-1}, shaded), 850–600-hPa ascent (blue, every 2.5 × 10^{-3} hPa s^{-1}), SLP (hPa, black), and 10-m wind (m s^{-1}, barbs)

Fig. 9

1200 UTC 11 Feb 2011

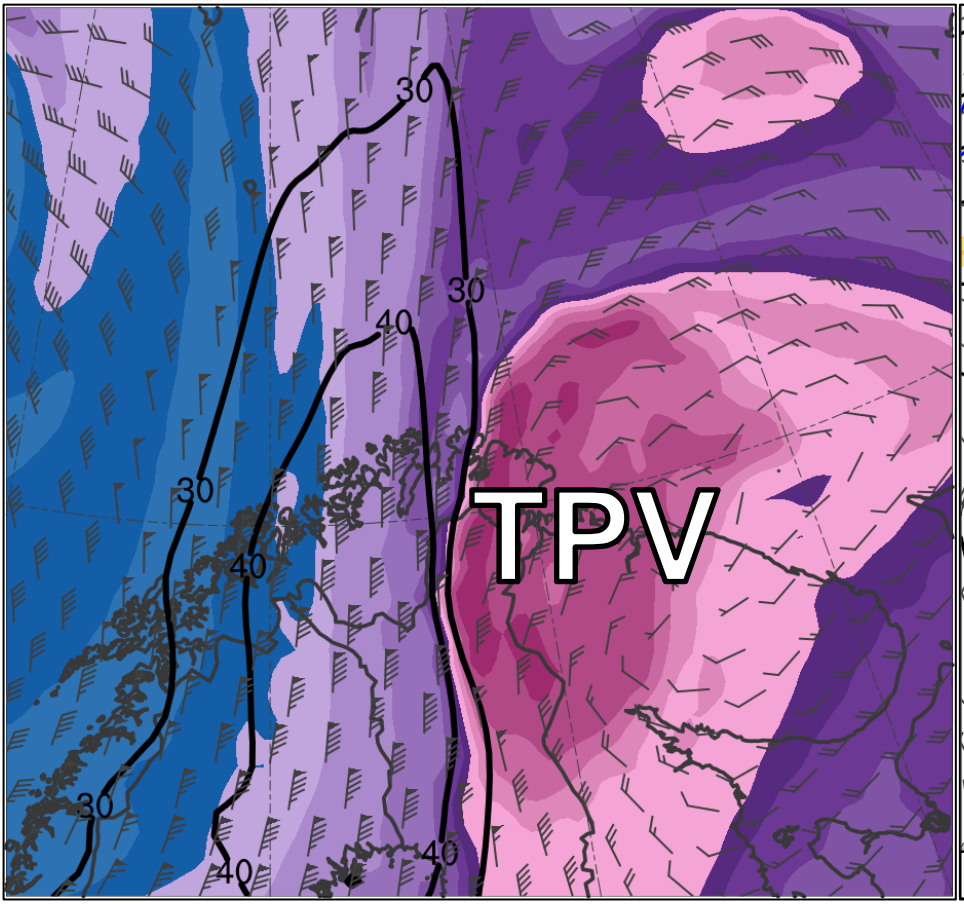

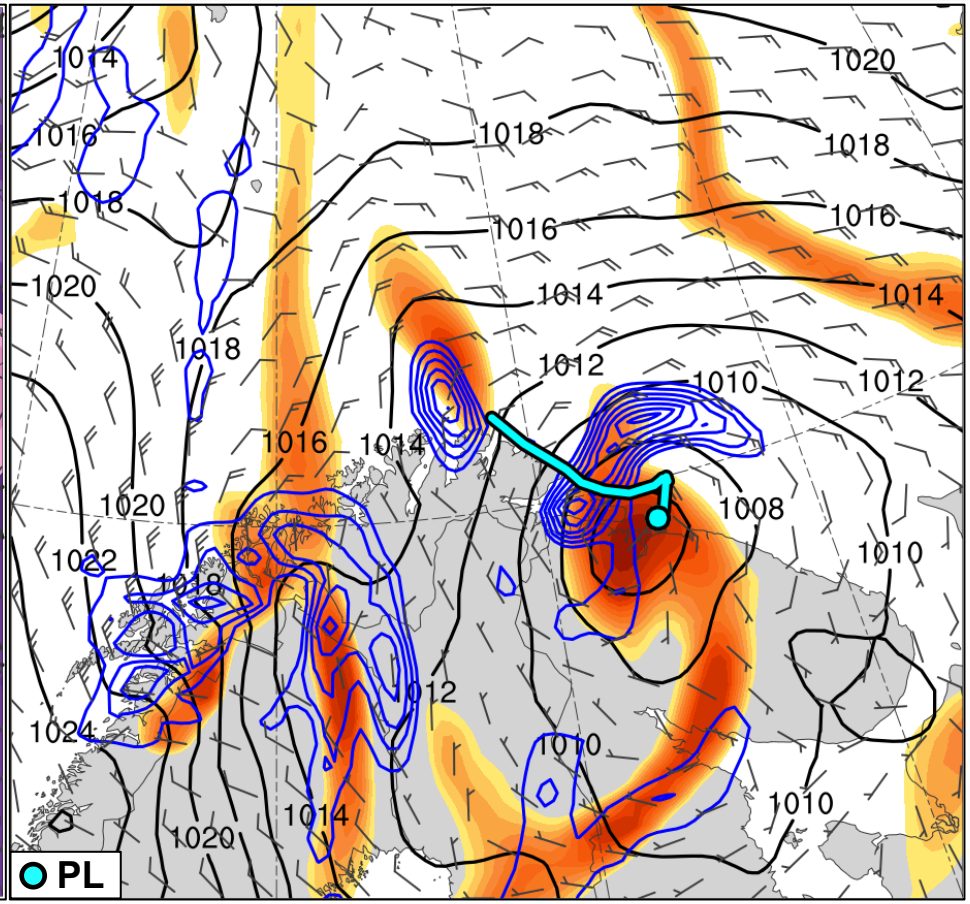

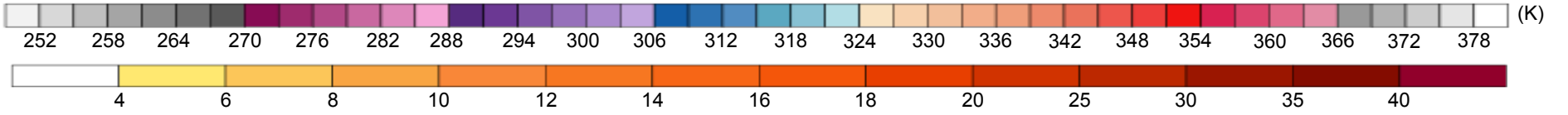

Potential temperature (K, shaded), wind speed (black, every 10 m s^{-1} starting at 30 m s^{-1}), and wind (m s^{-1}, flags and barbs) on 2-PVU surface

850-hPa relative vorticity (10^{-5} s^{-1}, shaded), 850–600-hPa ascent (blue, every 2.5 × 10^{-3} hPa s^{-1}), SLP (hPa, black), and 10-m wind (m s^{-1}, barbs)

Fig. 10

0300 UTC 11 Feb 2011

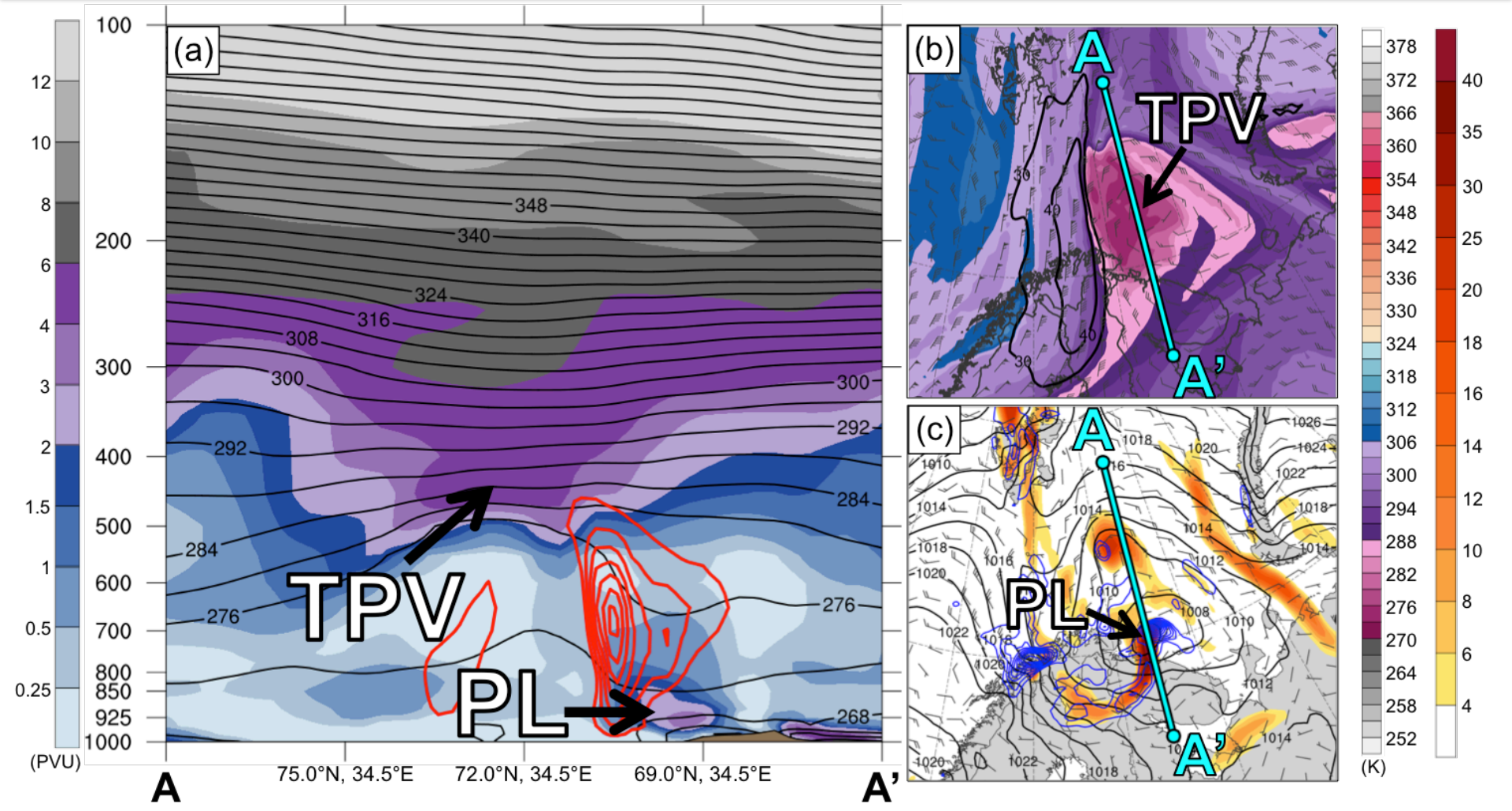

(a) PV (PVU, shaded), θ (K, black), and ascent (red, every 2.5 × 10^{-3} hPa s^{-1}); (b) DT (2-PVU surface) θ (K, shaded), wind speed (black, m s^{-1}), and wind (m s^{-1}, flags and barbs); (c) 850-hPa relative vorticity (10^{-5} s^{-1}, shaded), 850–600-hPa ascent (blue, every 2.5 × 10^{-3} hPa s^{-1}), SLP (hPa, black), and 10-m wind (m s^{-1}, barbs)

Fig. 11

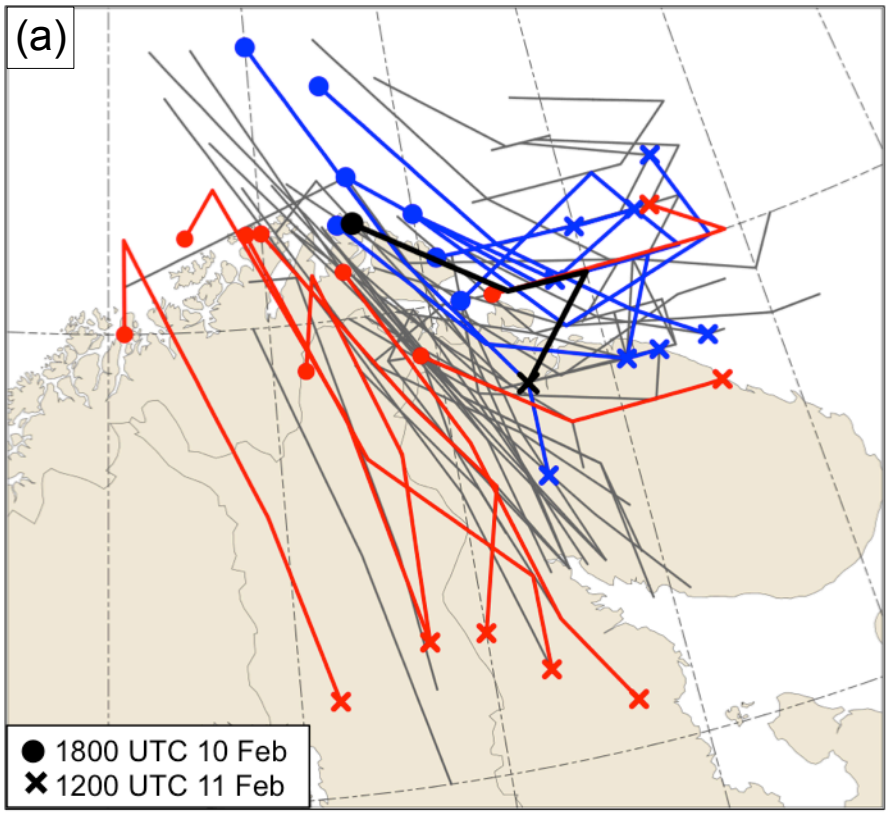

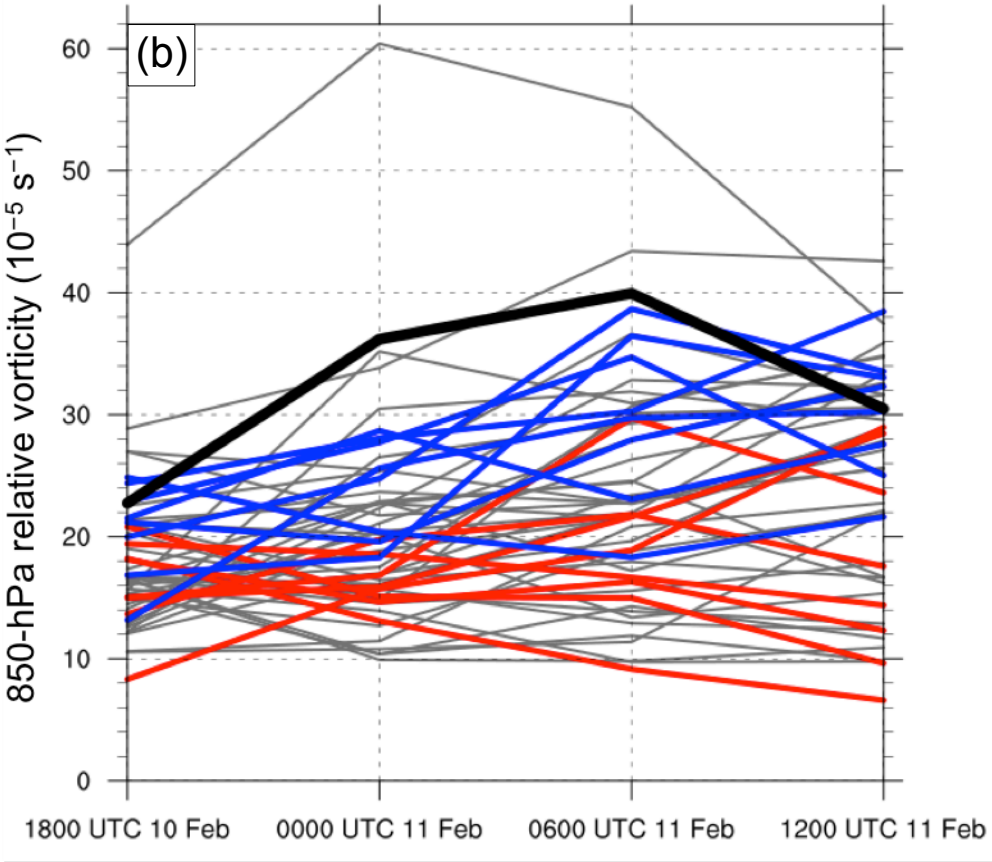

ERA5 — Most accurate members — Least accurate members — All other ECMWF EPS members

(a) Track and (b) intensity of 850-hPa relative vorticity maximum (10^{-5} s^{-1}) associated with polar low, every 6 h during 1800 UTC 10–1200 UTC 11 February 2011 for ERA5 (black), most accurate members (blue), least accurate members (red), and all other ECMWF EPS members (gray)

Supplementary Figures

Fig. 12

0000 UTC 8 Feb 2011

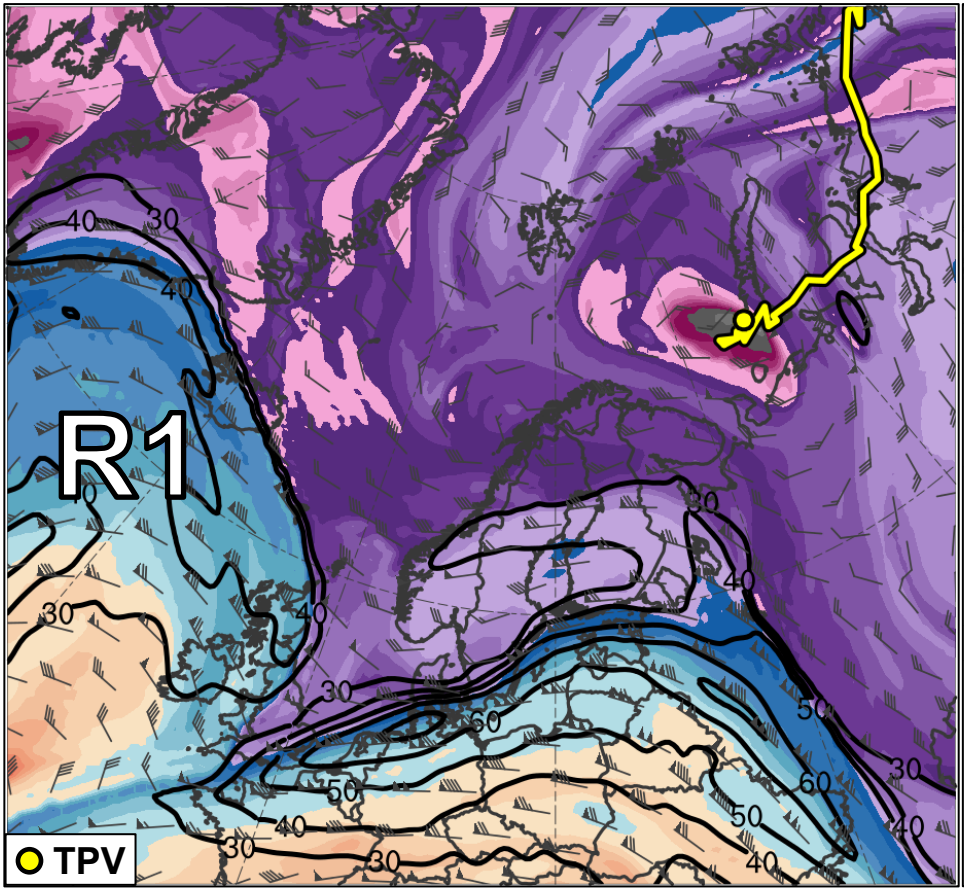

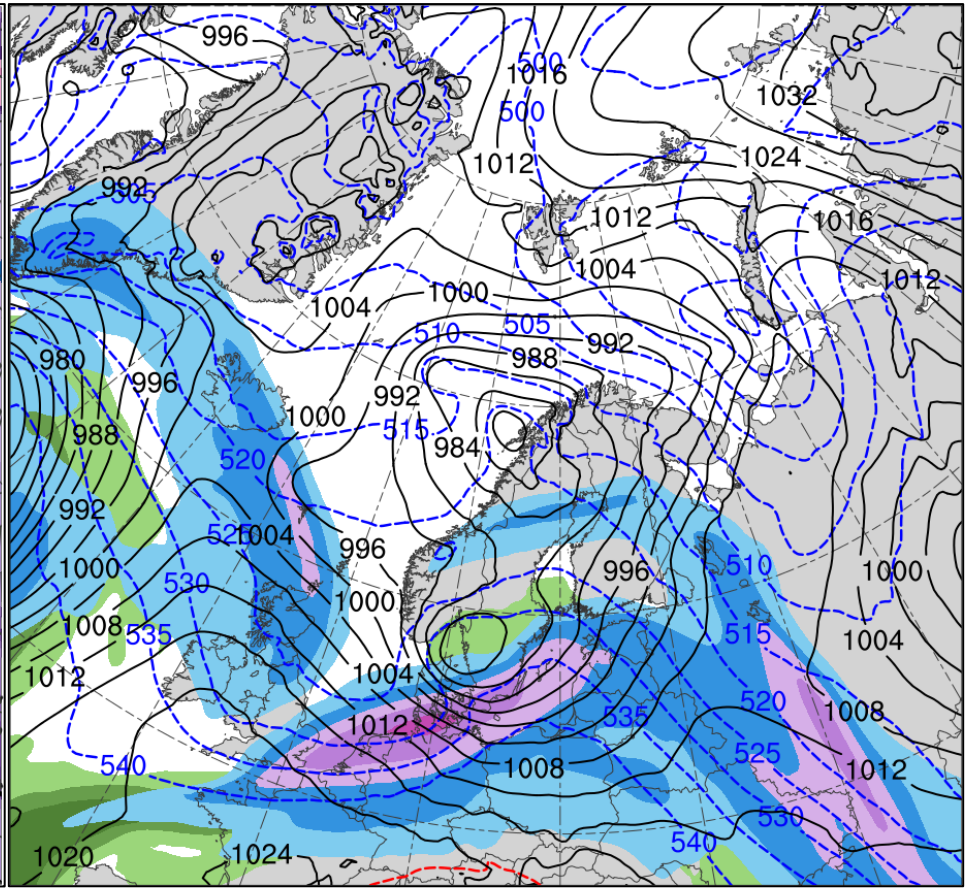

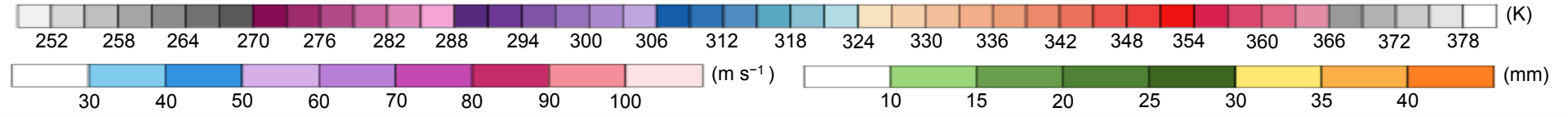

Potential temperature (K, shaded), wind speed (black, every 10 m s^{-1} starting at 30 m s^{-1}), and wind (m s^{-1}, flags and barbs) on 2-PVU surface

300-hPa wind speed (m s^{-1}, shaded), 1000–500-hPa thickness (dam, blue/red), SLP (hPa, black), and PW (mm, shaded)

Fig. 12

0000 UTC 9 Feb 2011

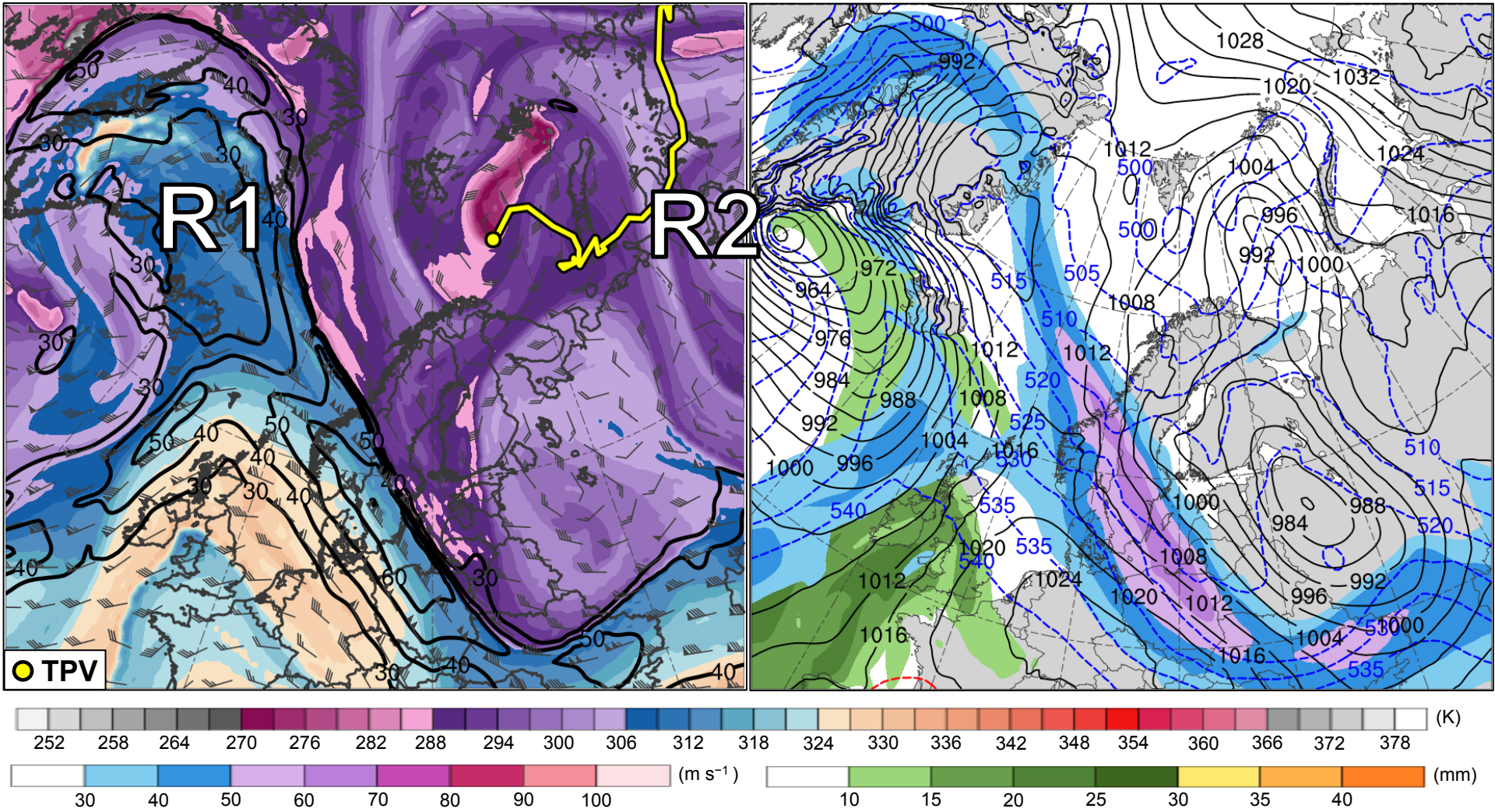

Potential temperature (K, shaded), wind speed (black, every 10 m s^{-1} starting at 30 m s^{-1}), and wind (m s^{-1}, flags and barbs) on 2-PVU surface

300-hPa wind speed (m s^{-1}, shaded), 1000–500-hPa thickness (dam, blue/red), SLP (hPa, black), and PW (mm, shaded)

Fig. 12

0000 UTC 10 Feb 2011

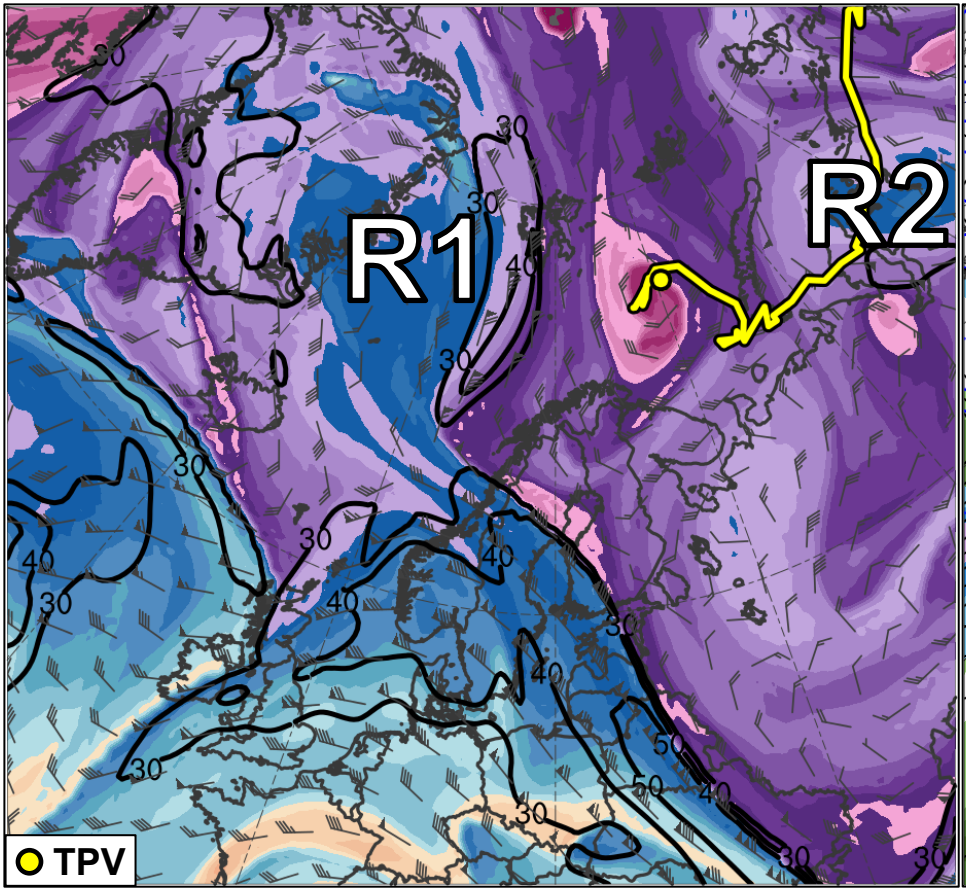

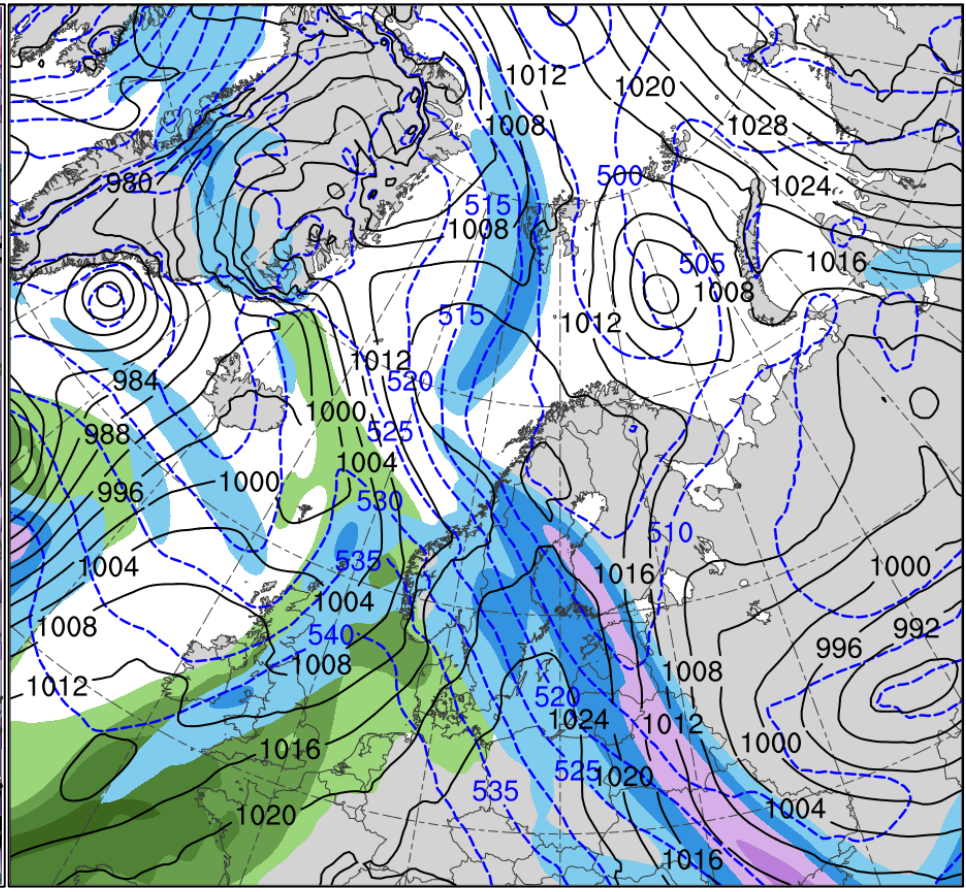

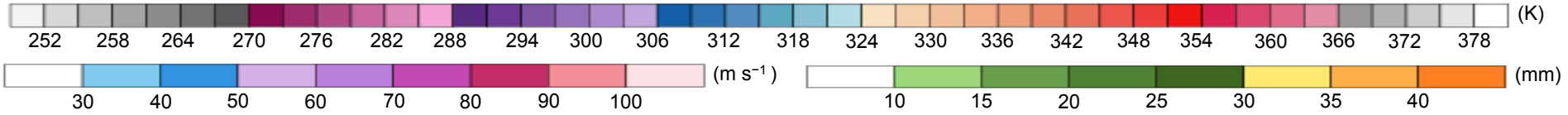

Potential temperature (K, shaded), wind speed (black, every 10 m s^{-1} starting at 30 m s^{-1}), and wind (m s^{-1}, flags and barbs) on 2-PVU surface

300-hPa wind speed (m s^{-1}, shaded), 1000–500-hPa thickness (dam, blue/red), SLP (hPa, black), and PW (mm, shaded)

Fig. 12

0000 UTC 11 Feb 2011

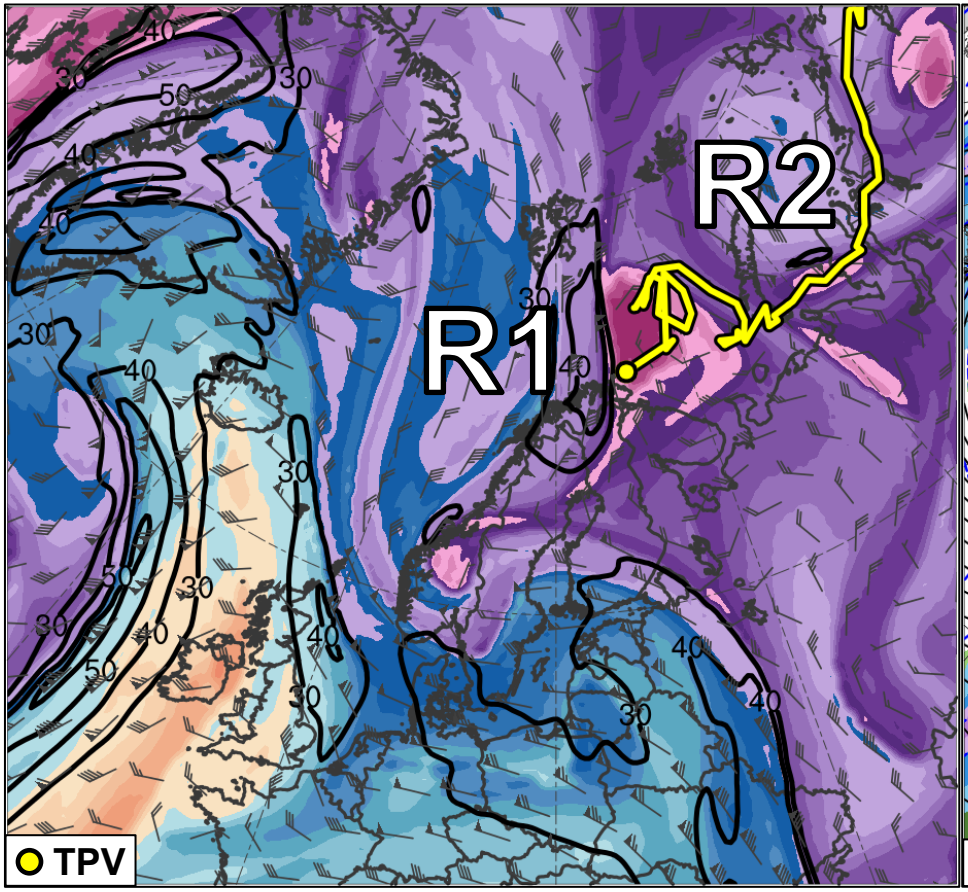

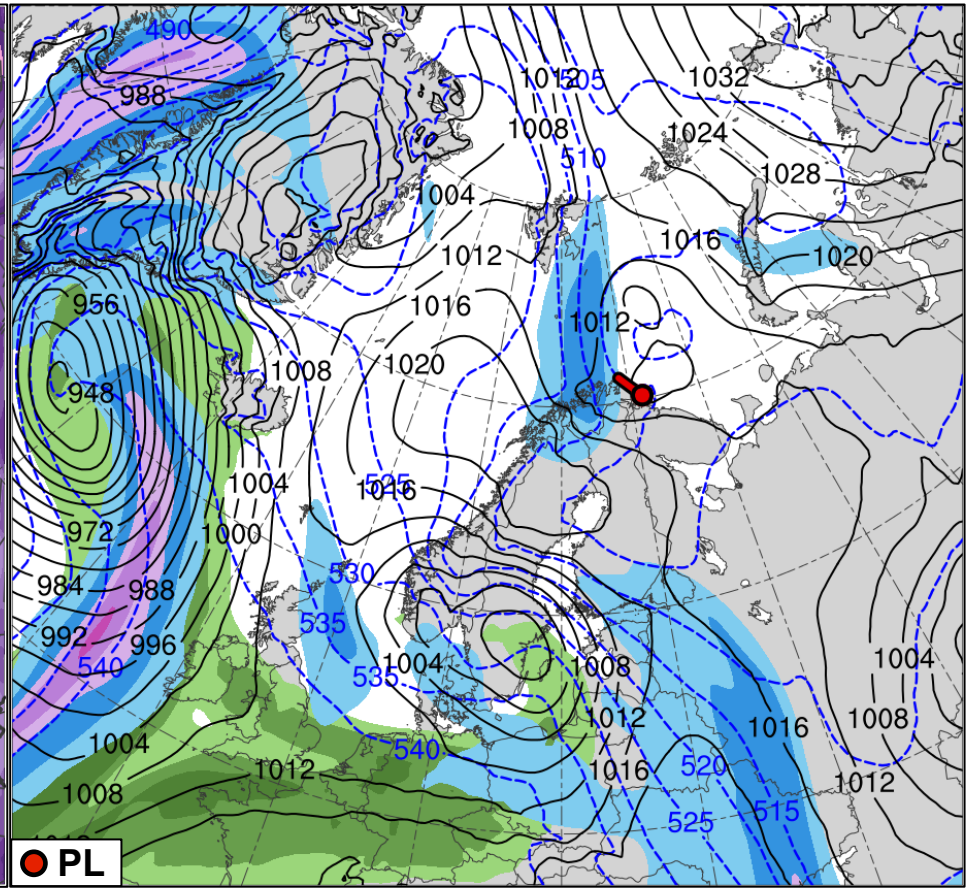

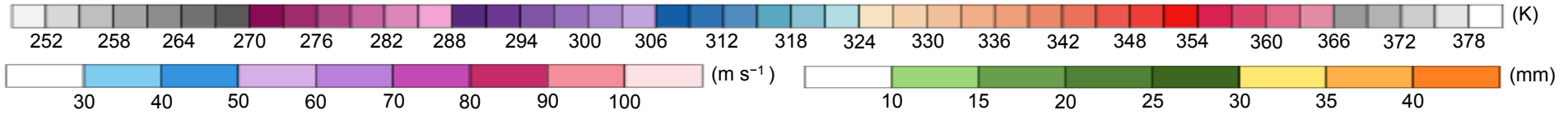

Potential temperature (K, shaded), wind speed (black, every 10 m s^{-1} starting at 30 m s^{-1}), and wind (m s^{-1}, flags and barbs) on 2-PVU surface

300-hPa wind speed (m s^{-1}, shaded), 1000–500-hPa thickness (dam, blue/red), SLP (hPa, black), and PW (mm, shaded)

Fig. 13

0300 UTC 11 Feb 2011

(a) SLP (hPa, blue), and 600–400-hPa layer-averaged **Q** (K m^{-1} s^{-1}, vectors), **Q** forcing for vertical motion (10^{-17} Pa^{-1} s^{-3}, shaded), geopotential height (dam, black), and potential temperature (°C, red)

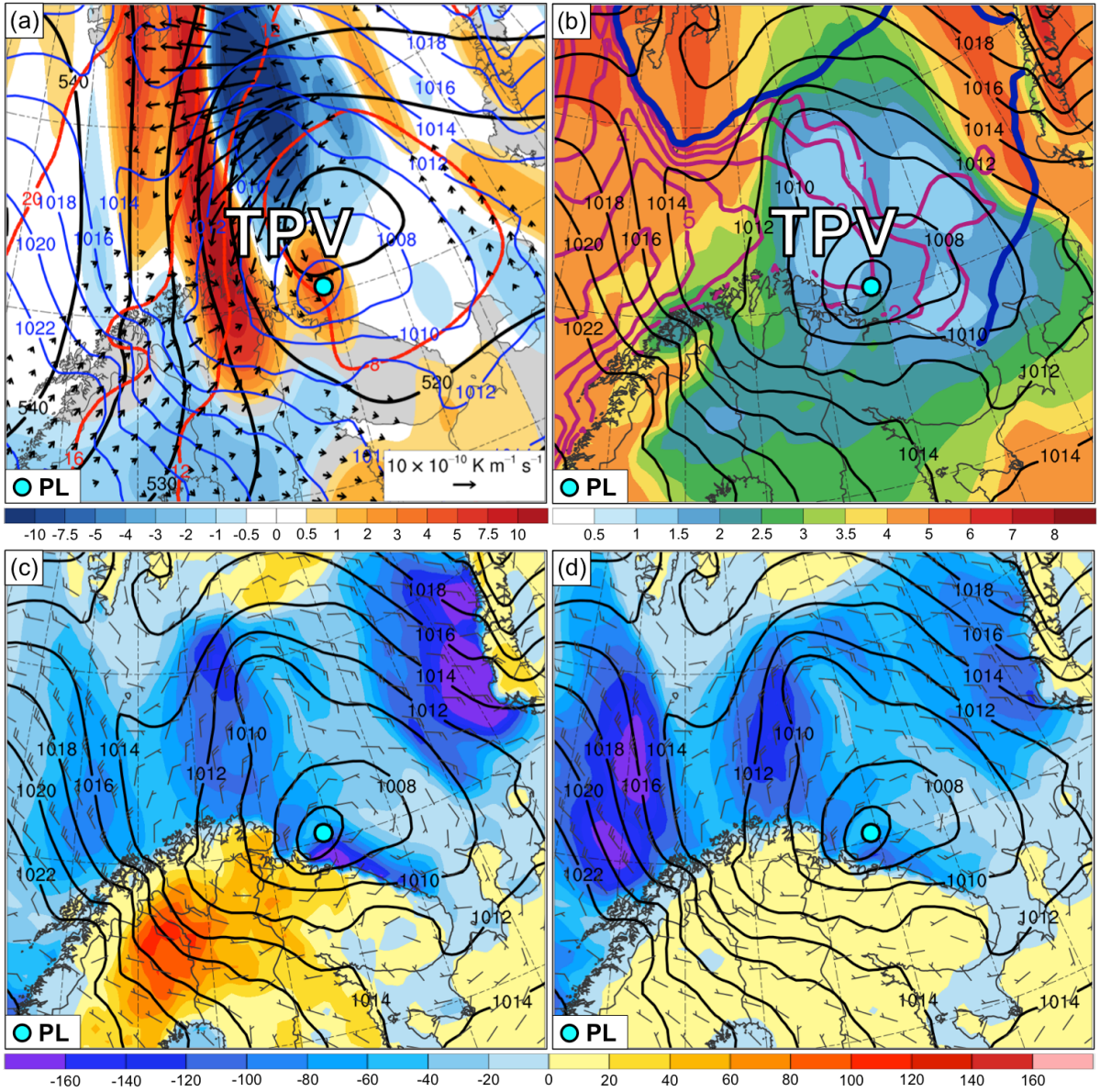

(b) 900–600-hPa layer-averaged static stability [K (100 hPa)$^{-1}$, shaded], SLP (hPa, black), SST (°C, purple), and 20% contour of sea-ice concentration (thick blue)

(c) SLP (hPa, black), 10-m wind (m s^{-1}, barbs), and sensible heat flux (W m^{-2}, shaded)

(d) SLP (hPa, black), 10-m wind (m s^{-1}, barbs), and latent heat flux (W m^{-2}, shaded)

Fig. 14

1800 UTC 10 Feb 2011 (30 h)

Ensemble mean

shading: normalized composite differences (most accurate minus least accurate)

stippling: statistically significant differences between groups at 95% confidence level

Mean position of PL in most accurate group*

Mean position of PL in least accurate group*

*Corresponding line shows mean track of PL from 1800 UTC 10 to 1200 UTC 11 Feb 2011

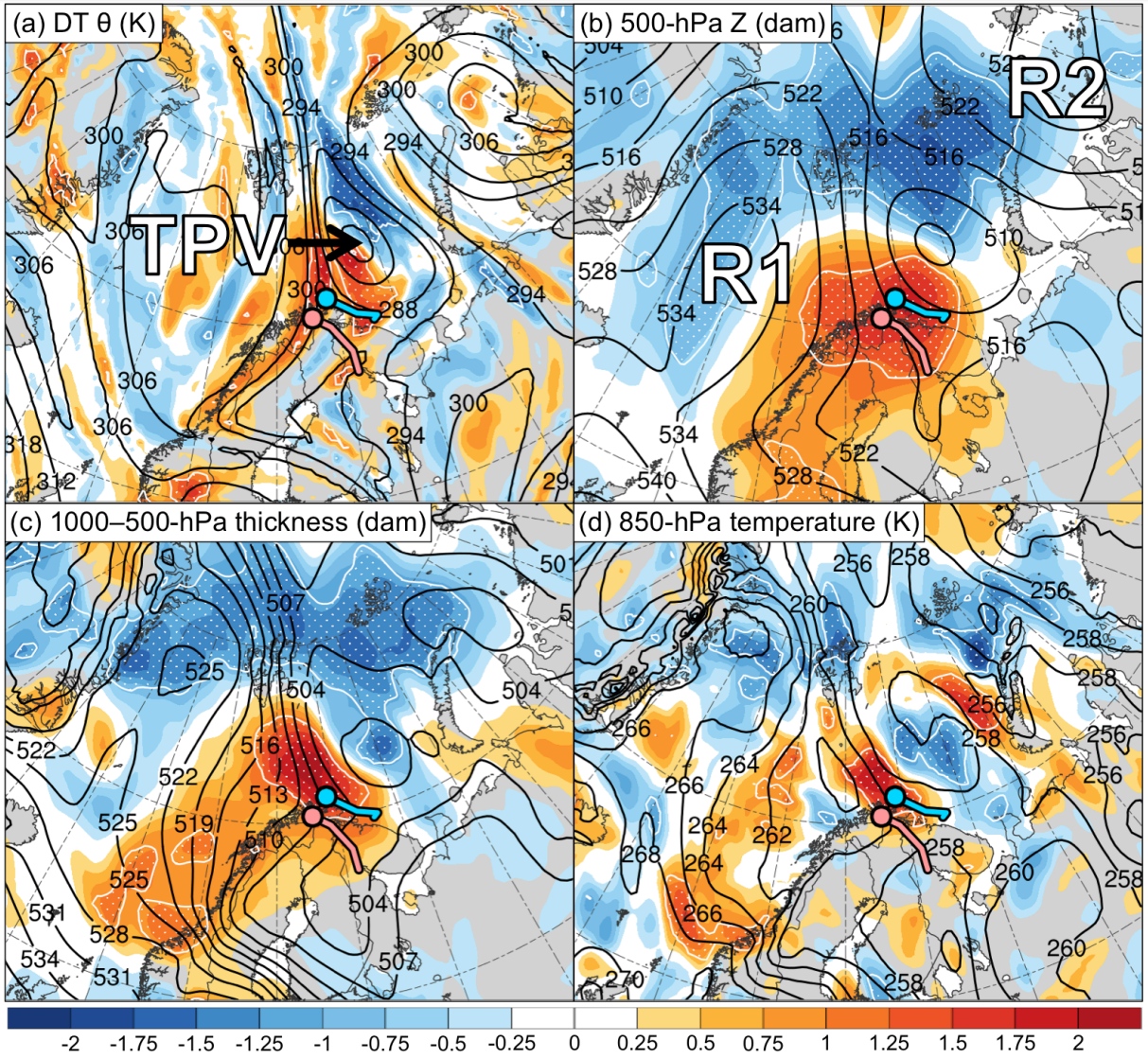

Normalized composite difference between the most accurate and least accurate group (shading; units: standardized anomaly) and ensemble mean (black contours) of (a) DT (2-PVU surface) potential temperature (K), (b) 500-hPa geopotential height (dam), (c) 1000–500-hPa thickness (dam), and (d) 850-hPa temperature (K).